Version 2.0
October, 2003

Wide Field Camera 3 Instrument Mini-Handbook for Cycle 13

Available in Cycle 14
Do not propose for WFC3 in Cycle 13

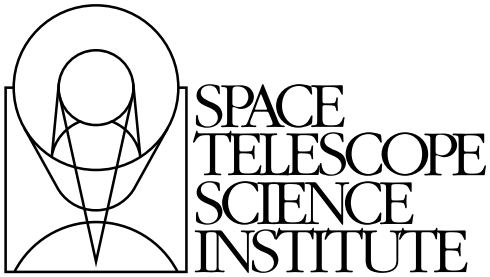

Space Telescope Science Institute
3700 San Martin Drive
Baltimore, Maryland 21218
help@stsci.edu

Operated by the Association of Universities for Research in Astronomy, Inc., for the National Aeronautics and Space Administration

User Support

For prompt answers to any question, please contact the STScI Help Desk.

- **E-mail:** help@stsci.edu
- **Phone:** (410) 338-1082
  (800) 544-8125 (U.S., toll free)

World Wide Web

Information and other resources are available on the WFC3 World Wide Web sites at STScI and GSFC:

- **URL:** http://www.stsci.edu/instruments/wfc3
- **URL:** http://wfc3.gsfc.nasa.gov

WFC3 History

Version	Date	Editor
1.0	October 2002	Mauro Giavalisco
2.0	October 2003	Massimo Stiavelli

Contributors:

Sylvia Baggett, Wayne Baggett, Howard Bushouse, Mauro Giavalisco, Shireen Gonzaga, Christopher Hanley, Bryan Hilbert, Ray Kutina, Olivia Lupie, John MacKenty, Neill Reid, Massimo Robberto, Michael Robinson, Massimo Stiavelli.

Citation:

In publications, refer to this document as:
Stiavelli, M., et al. 2003 "Wide Field Camera 3 Instrument Mini-Handbook", Version 2.0, (Baltimore: STScI).

Send comments or corrections to:
Space Telescope Science Institute
3700 San Martin Drive
Baltimore, Maryland 21218
E-mail:help@stsci.edu

Acknowledgments

The WFC3 Science Integrated Product Team

Sylvia Baggett
Wayne Baggett
Howard Bushouse
Randy Kimble (Instrument Scientist, GSFC)
Christopher Hanley
Robert Hill (GSFC)
Bryan Hilbert
Ray Kutina
Olivia Lupie
John MacKenty (Deputy Instrument Scientist)
Neill Reid
Massimo Robberto (ESA-STScI)
Michael Robinson
Massimo Stiavelli

The WFC3 Science Oversight Committee

Bruce Balick, University of Washington
Howard E. Bond, Space Telescope Science Institute
Daniela Calzetti, Space Telescope Science Institute
C. Marcella Carollo, Institute of Astronomy, ETH, Zurich
Michael J. Disney, University of Wales
Michael A. Dopita, Mt Stromlo and Siding Springs Observatories
Jay Frogel, Ohio State University (former member, on leave NASA HQ)
Donald N. B. Hall, University of Hawaii
Jon A. Holtzman, New Mexico State University
Gerard Luppino, University of Hawaii
Patrick J. McCarthy, Carnegie Observatories
Robert W. O'Connell, University of Virginia (Chair)
Francesco Paresce, European Southern Observatory
Abhijit Saha, National Optical Astronomy Observatory
Joseph I. Silk, Oxford University
John T. Trauger, Jet Propulsion Laboratory

Alistair R. Walker, Cerro Tololo Interamerican Observatory
Bradley C. Whitmore, Space Telescope Science Institute
Rogier A. Windhorst, Arizona State University
Erick T. Young, University of Arizona

Acknowledgments

The Editor wishes to thank all members of the WFC3 Science Integrated Product Team who have generously helped in various ways.

Table of Contents

Wide Field Camera 3

In this book. . .

1. Overview

1.1 General

The Wide Field Camera 3 (WFC3) is a fourth-generation instrument to be installed on the Hubble Space Telescope (HST) during Servicing Mission 4 (SM4), currently scheduled for late 2004. The instrument will occupy one of the HST radial bays, where it will replace WFPC2, which will have served on orbit for over 10 years by 2004. WFC3 is designed to ensure that HST maintains its unique imaging capabilities until the end of its mission, while at the same time advancing its survey and discovery capability due to its combination of wavelength coverage, field of view, and sensitivity. WFC3 will also provide a good degree of redundancy for ACS and NICMOS.

WFC3 is a facility instrument, and unlike the other HST instruments, it is being built by NASA through a partnership between the NASA Goddard Space Flight Center (GSFC), Space Telescope Science Institute (STScI), Ball Aerospace, and other industrial contractors. Specifically, definition of the instrument, design, construction, testing, characterization and calibration of WFC3 are not carried out by an Investigation Definition Team (IDT) under the leadership of a Principal Investigator (PI) selected by NASA, as traditionally done in the past, but rather they are the responsibilities of an Integrated Product Team (IPT) led by GSFC and composed of staff astronomers and engineers from GSFC, STScI, Jet Propulsion Laboratories (JPL), Ball Aerospace, and industrial contractors.

A Science Oversight Committee (SOC) selected by NASA from the worldwide astronomical community provides scientific oversight of the design and development of WFC3 to ensure that its scientific capabilities are adequate to serve as a facility instrument until the end of the HST mission. The SOC has provided important scientific input in a variety of areas, such as defining the suite of filters for WFC3, and continues to provide scientific advice on major design trade decisions.

1.2 Key Features of Wide Field Camera 3

The optical design of WFC3 features two independent channels, one sensitive at ultraviolet (UV) and optical wavelengths, approximately 200 to 1000 nm (the UVIS channel), and the other sensitive at near infrared (IR) wavelengths, approximately 850 to 1700 nm (the IR channel). A channel-selection mechanism consisting of a movable mirror directs the light coming from the HST Optical Telescope Assembly (OTA) to one of the two selected channels, and hence no simultaneous observations with UVIS and IR are possible.

The extended wavelength range combines with high sensitivity, angular resolution, large field of view, and wide selection of spectral elements to make WFC3 one of the most versatile instruments on board HST. Key features of the instrument include:

- UVIS channel: 0.04 arcsec/pix; 2.7x2.7 arcmin FOV; 200-1000 nm; point source with V=29.1 at S/N=5 in 10 hr.
- IR channel: 0.13 arcsec/pix; 2.1x2.3 arcmin FOV; 850-1700 nm; point source with H=26.3 at S/N=5 in 10 hr.
- 62 broad-, medium-, and narrow-band filters in the UVIS channel.
- 15 broad-, medium-, and narrow-band filters in the IR channel.
- 1 grism in the UVIS channel, and 2 grisms in the IR channel, for slitless spectroscopy.
- IR detector with reference pixels for accurate bias subtraction.

A White Paper document (Stiavelli, M. and O'Connell, R.W. eds. 2000, "Hubble Space Telescope Wide Field Camera 3, Capabilities and Scientific Program") prepared by the SOC and the science IPT outlines the scientific areas that will most benefit from the specific capabilities of WFC3. These include searches for galaxies at redshift up to z~10, the study of the physics of star formation in distant and nearby galaxies, accurate determination of the baryonic mass by detecting stars at the limit of the hydrogen-burning sequence and extra-solar Jupiter-like planets, and study of planetary objects in the Solar System. The document can be found at:

http://wfc3.gsfc.nasa.gov/white_paper.html

1.3 The WFC3 Instrument Team at STScI

STScI maintains a team of Instrument Scientists, Data Analysts, Engineers, and Scientific Programmers who support the design, development, operation, calibration and documentation of WFC3. STScI also maintains a Help Desk to provide answers quickly to any WFC3- and HST-related questions. Please send all questions regarding WFC3 and HST to the Help Desk. To contact the Help Desk at STScI:

- Send E-mail to: help@stsci.edu
- Phone: (410) 338-1082

2. Instrument Description

2.1 Optical Design

The optical design of WFC3 was driven by the need to provide a large field of view and high sensitivity over a broad wavelength region, excellent spatial resolution, and stable and accurate photometric performance. WFC3 features two independent imaging cameras, the UV/optical channel (UVIS) and the near-infrared channel (IR), as illustrated in Figure 1, which shows a schematic of the optical layout of the instrument. The UVIS channel uses 2 butted 4096x2051 thinned, back-illuminated Marconi CCD detectors to support imaging between 200 and 1000 nm, while the IR channel uses a 1024x1024 Rockwell HgCdTe detector array, with 1014x1014 pixels useful for imaging, to cover between 850 and 1700 nm. A flat pick off mirror redirects the beam coming from the HST Optical Telescope Assembly (OTA) into WFC3, and both channels produce images centered around the same on-axis line-of-sight in the HST focal plane, but not simultaneously; a channel-select mechanism is included to divert the light to the desired channel. Optical elements in each channel correct for the spherical aberration of the HST primary mirror. The primary characteristics of the two channels are summarized in Table 1.

Table 1: Summary of the primary characteristics of the two channels of WFC3.

Channel	Field of View (size in arcsec)	Average scale, in arcsec	Spectral range, in nanometers	Detector pixel format
UVIS	163x162	0.040 x 0. 040	200-1000	2x4096x2048
IR	123x137	0.121 x 0.135	850-1700	1014x1014

The UVIS channel is similar to the Wide Field Camera (WFC) of the Advanced Camera for Surveys (ACS). There are, however, some differences that make it unique. UVIS provides about 20% better spatial sampling than ACS/WFC, obtained at the price of a comparably smaller field of view. Furthermore, while ACS/WFC is blind at wavelengths shorter than approximately 370 nm (namely, bluer than the B band), WFC3 UVIS has sensitivity that extends to the UV spectral region, covering the range from 200 nm to 1000 nm; however, the design trade-offs adopted to achieve such an extended wavelength coverage (primarily the coating of the CCD and the use of aluminum for the M1 and M2 mirrors; see Figure 1) imply a reduced sensitivity at optical wavelengths compared to that of ACS/WFC. In the UV spectral region, WFC3/UVIS has better near-UV throughput and much larger field of view than ACS/HRC, although it has coarser spatial sampling. WFC3/UVIS is not sensitive in the far-UV region (i.e. wavelengths shorter than 200 nm); this is covered by ACS/SBC and STIS/FUV-MAMA. WFPC2 has some sensitivity at wavelengths shorter than 200 nm but it will be physically replaced by WFC3 and thus it will be unavailable.

The IR channel offers 85% of the imaging area of the Wide Field Planetary Camera 2 (WFPC2) with only ~30% larger pixel size. It covers about 7 times the area of the Near Infrared Camera and Multi Object Spectrometer (NICMOS) NIC3 channel with almost 2 times better spatial sampling, but it lacks the very high sampling offered by the NICMOS/NIC1 channel. WFC3 also provides improved sensitivity over NICMOS, although its wavelength coverage is smaller, ending at about 1700 nm, to limit the instrument's thermal background. This is due to the fact that, unlike NICMOS, the IR channel does not have a cryogenic dewar that cools many components of the instrument; instead, various parts of WFC3, including the optical bench, Refractive Corrector Plate (RCP), pupil mask, baffle, and detector container, are actively cooled by a thermal-control subsystem, each at its optimal temperature. Although much simpler, this design does not provide for adequate suppression of the thermal background at wavelengths longer than the H band and limits the detector temperature to ~150 K. Each channel includes a calibration subsystem that provides internal illumination of the detector for flat-field calibrations.

Figure 1: Schematic of the optical layout of the WFC3 instrument.

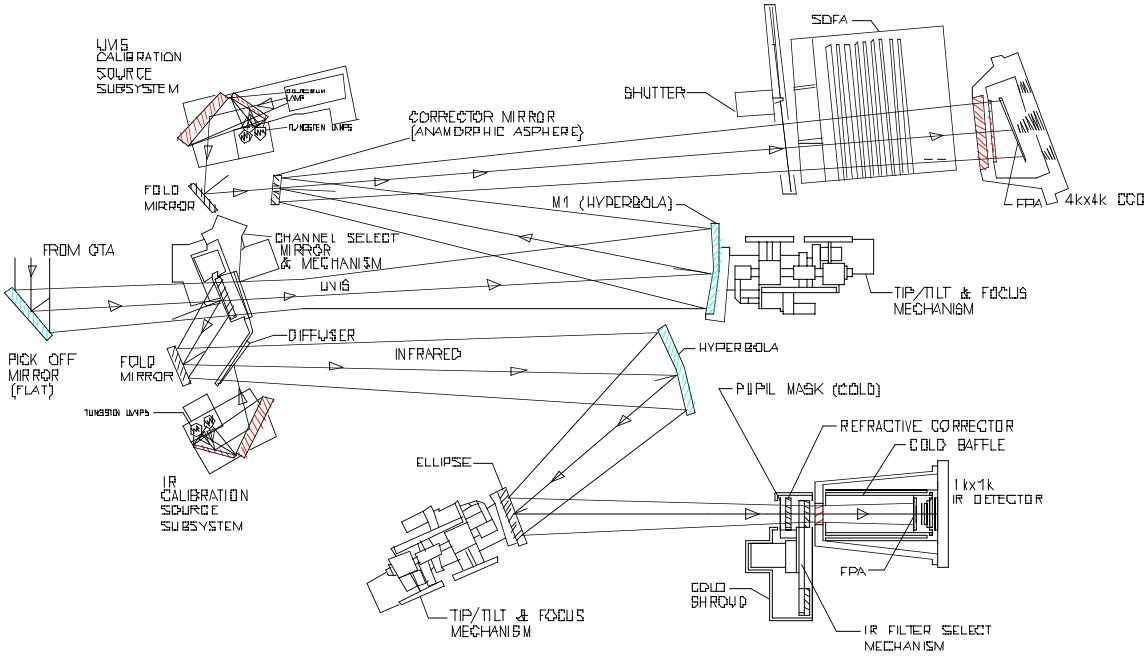

Table 2: A comparison of the primary characteristics of HST imaging instruments.

Instrument	Wavelength coverage, nanometers	Pixel size, arcsec	Area Coverage, square arcmin
WFC3 UVIS	**200 – 1100**	**0.04**	**7.335**
ACS WFC	370 – 1100	0.05	11.67
ACS HRC	200 – 1010	0.025	0.174
ACS SBC	115 – 170	0.03	0.25
STIS FUV-MAMA	115 – 170	0.024	0.174
STIS NUV-MAMA	160 – 310	0.024	0.174
STIS CCD	200 – 1100	0.05	0.404
WFPC2 WF	115 – 1100	0.10	5.333
WFPC2 PC	115 – 1100	0.046	0.444
WFC3 IR	**850 – 1700**	**0.13**	**4.681**
NICMOS NIC1	850 – 2500	0.043	0.0336
NICMOS NIC2	850 – 2500	0.075	0.100
NICMOS NIC3	850 – 2500	0.20	0.728

Table 2 shows a comparison of the wavelength coverage, pixel scale and field of view of present HST imaging cameras and WFC3, while Figure 2 shows the expected throughput of WFC3 as a function of wavelength

compared to that of WFPC2, ACS, and NICMOS. The curves include the multiplicative contribution of the individual throughput of the OTA, all the optical elements of the instruments themselves (excluding filters but including the detectors' windows), and the sensitivity of the detectors. The thick continuous WFC3 curves are obtained using the currently selected flight detectors As the figure shows, WFC3 offers a unique combination of high sensitivity and wide spectral coverage ranging from the UV to the near-IR. WFC3 extends and complements over a large field of view the optical performance of ACS/WFC at wavelengths shorter than ~400 nm and longer than 1000 nm. The good degree of functional redundancy with ACS and NICMOS will help ensure that the unique scientific capabilities of HST will remain available until the end of its mission.

Figure 2: The integrated system throughput of imaging instruments on HST as a function of wavelength. The thick continuous curves represent the performance of WFC3 with the currently selected flight detectors. The dashed curves represent the throughput of ACS, WFPC2 and NICMOS.

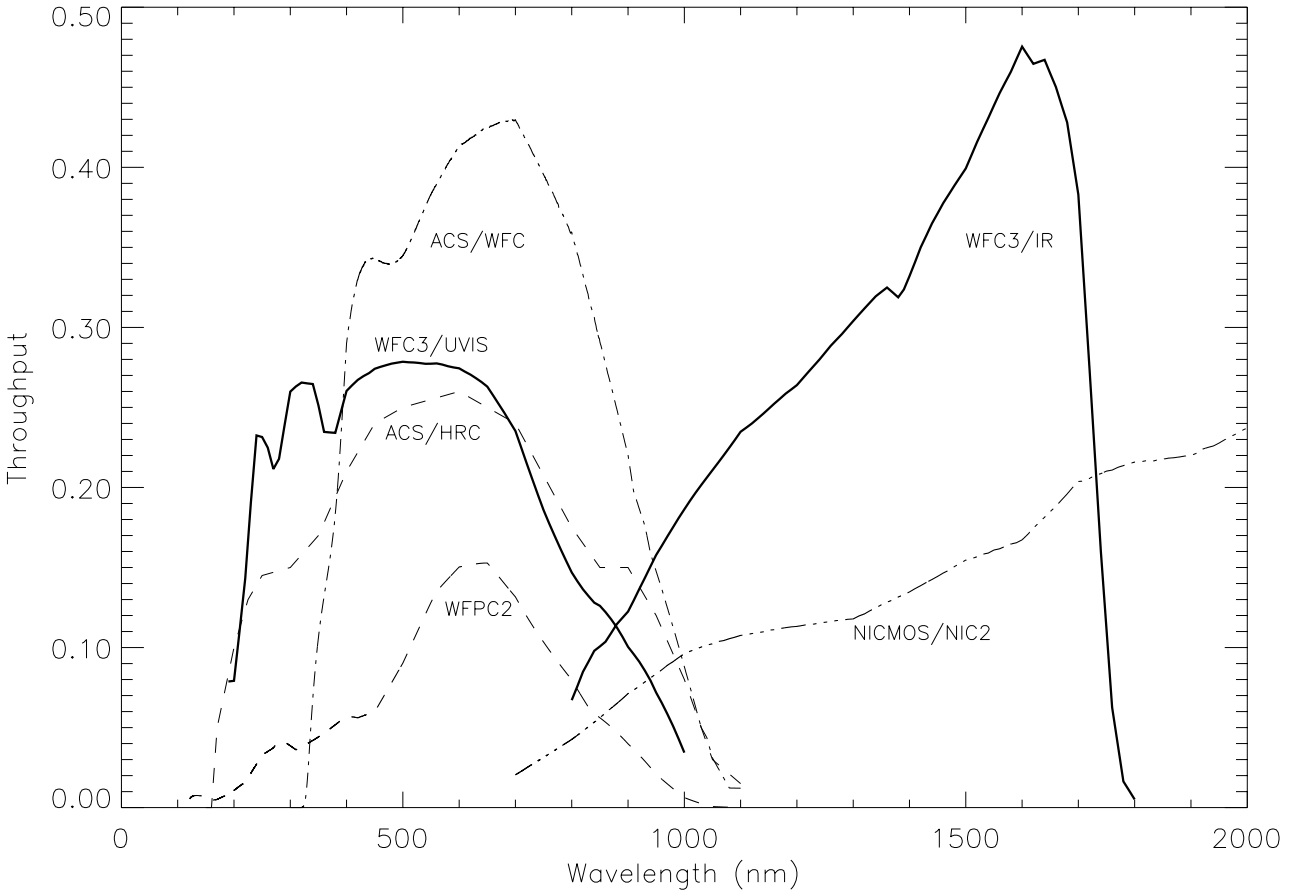

WFC3 will replace WFPC2, the first large-area camera that included corrections for the spherical aberration on HST. The appearance of the HST focal plane following the Fourth Servicing Mission is shown in Figure 3. Similar to ACS, the imaging areas of WFC3 are subject to geometrical distortions as a result of a focal plane tilt in the optical design which elongates the field of view by a small amount. Most of the distortion runs approximately parallel to the diagonal direction of the UV detector and

parallel to the axis of the IR one. As a result, the UVIS aperture on the sky will look like a rhombus with the acute angle between the x and y axes of the detector being approximately 86 degrees, while the IR channel aperture will be rectangular in shape with an aspect ratio of about 89%. The pixel scale of the two channels is approximately 0.040 and 0.13 arcsec/pixel, respectively (see Table 1 and Section 3).

Both channels are complemented with a large collection of spectral elements, selected after the recommendations of the SOC following the results of a Filter Selection Workshop held at STScI on July 14, 1999. The collection includes broad-, medium-, and narrow-band filters as well as low-dispersion grisms (one element in the UVIS channel and two in the IR channel) for slitless spectroscopy. The broad-band filters include popular passbands frequently used in extragalactic and stellar astronomy, as well as passbands used in other HST instruments for photometric consistency. A total of 36 different narrow-band passbands consisting of 16 normal filters and 5 QUAD filters sample throughout the UVIS channel spectral range, including filters that target the most important spectroscopic features. The IR channel includes 6 narrow-band filters also targeting the most important spectral features in the near IR. Unlike ACS or WFPC2, no ramp filters or polarizers are included. Finally, broad-band filters with similar wavelength coverage as that of the dispersers are available to observers for obtaining direct images of their spectroscopic targets in the same spectral region covered by the dispersed images, thus allowing accurate identification of the sources and wavelength calibration. Table 4 and 5 list the spectral elements of the UVIS and IR channel, respectively, divided by type.

Both channels offer sub-arrays, and the UVIS allows binned readout modes, increasing the flexibility of observing configurations. A variety of dithering schemes is offered to observers by the APT proposal software tools, including specially designed patterns as well as user-defined ones. The post-observation software (pipeline) calibrates data taken in all these configurations and also offers the option of reconstructing dithered images with the drizzling algorithm, effectively increasing the sampling of the Point Spread Function (PSF). The software also handles mosaic images according to a set of rules or associations and regrids them onto a cartesian pixel coordinate system.

Figure 3: The layout of the focal plane of HST after SM4.

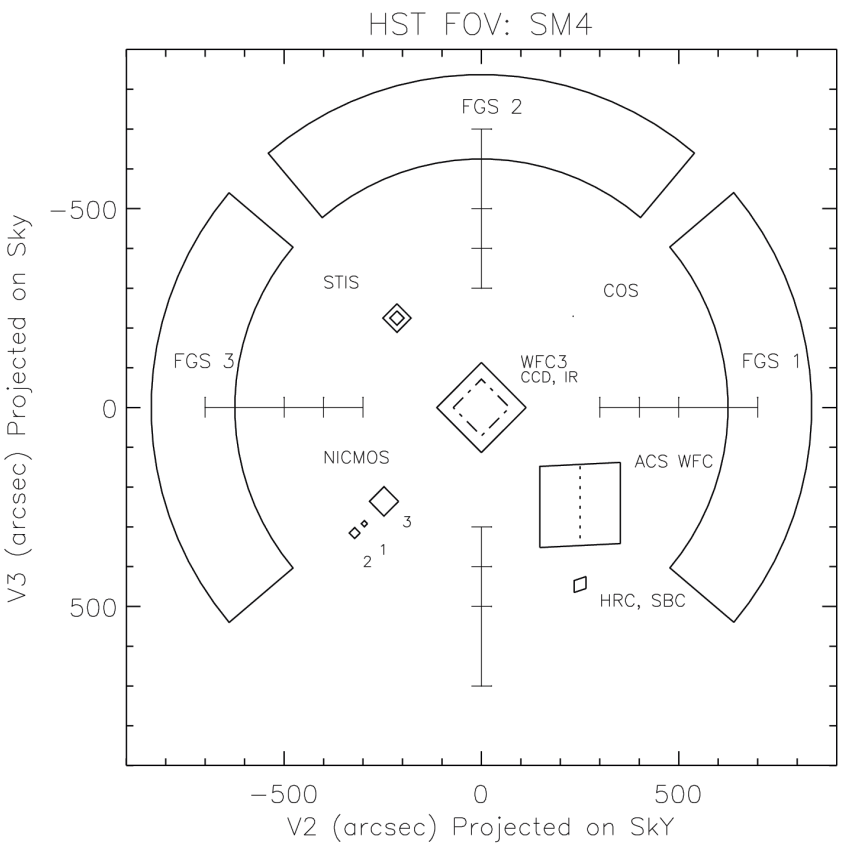

3. The UVIS Channel

The UVIS channel is optimized for highest performance in the 200 – 400 nm wavelength interval, and consists of an optical train providing focus and alignment adjustment as well as correction for the HST Optical Telescope Assembly (OTA) spherical aberration, a filter element selection mechanism, a shutter, and a CCD detector assembly. These are supported by a thermal control subsystem and also by control and data-handling electronic subsystems. The UVIS channel contains a shutter mechanism, similar to that used in the ACS WFC. In concept and functionality, as well as in many design details, UVIS is patterned after the ACS/WFC channel.

3.1 Field of View and Pixel Size

The field of view of WFC3 is limited by the size of the pick-off mirror (POM), which is constrained to avoid vignetting of other science instruments. The UVIS channel adopts the same ACS/WFC camera-head design with 4096 x 4102 pixels in the focal plane. The projected pixel shape is not perfectly square, and the average value of the two scales are 0.0397 and 0.0395 arcsec/pixel, which yields a field of view of 163x162 arcsec. This exploits the available field of view while providing good sampling of the PSF in the visible.

3.2 CCD Detector

The UVIS channel has a focal plane populated by two 4096 x 2048 pixel CCDs butted together to yield a total of 4096 x 4096 array; the gap between the two chips is approximately 50 pixels (2 arcsec) wide. The CCDs are thinned, back-illuminated Marconi devices with UV-optimized anti-reflection coatings. As shown in Figure 2, their sensitivity extends to 200 nm while remaining relatively high in the visible and near-IR wavelengths. The optics are UV-optimized and the sensitivity in the range 200-350 nm is achieved by employing aluminum mirrors with magnesium fluoride (MgF2) coatings. This design works well in the red part of the spectrum too, where it yields a reflectivity of ~88% and enables WFC3 to reach a final throughput in the R band equal to ~50% that of ACS/WFC, including 3 internal reflections (see Figure 1) and the QE of the CCD detector. To achieve maximum sensitivity, the detector readout noise is expected to be less than 4 electrons rms and the dark current less than 10 electrons per pixel per hour. Such low values allow background-limited observations in broad-band filters at visible and longer wavelengths in single 1-orbit long exposures.

Accurate photometric performance requires uniform response within each pixel and excellent charge-transfer efficiency (CTE), which must be stable over a relatively long lifetime in the high-radiation environment where HST operates. The non-optimal CTE characteristics of WFPC2 at launch and their further degradation on orbit have been an important limitation for highly accurate photometry. The performance of the WFC3 CCD detectors has been improved by providing shielding to the CCD (same as ACS/WFC and similar to WFPC2) and designing the CCD with a mini-channel (improved over ACS/WFC), which will reduce the number of traps seen by small charge packets. In addition, WFC3 is the first HST instrument to include charge injection in order to mitigate the effects of CTE losses in the later years by increasing the background level to fill in traps without an excessive increase in the noise level of the images.

Another important detector parameter is the modulation transfer function (MTF), which defines how accurately a detector responds to a

signal rapidly changing in its spatial distribution (high frequency response). This depends on the uniformity of response within a pixel, which determines the potential photometric accuracy, and on the cross-talk between pixels, which degrades the PSF sharpness. Limits to the MTF of UVIS CCDs result in less than 10 per cent degradation of the PSF width over the whole spectral range of the channel, and better than 2 percent photometry in the visible.

3.3 Spectral Elements

The UVIS channel makes use of the refurbished WF/PC Selectable Optical Filter Assembly (SOFA) unit, which has 48 available slots. The slots accommodate 42 narrow, medium and broad-band filters, one UV grism, and 5 quad filters (4 filters in a 2 by 2 mosaic configuration), bringing the total to 63 individual spectral elements spanning the wavelength region 200-1000 nm. Table 4 lists all the available spectral elements, which include very broad-band filters for the deepest possible imaging, filters which match the most commonly used filters on WFPC2 to provide continuity with previous observations, the SDSS filters (also included in the ACS WFC collection), filters which are optimized to provide maximum sensitivity to various stellar parameters (e.g. the Stroemgren and Washington systems), and narrow-band filters which probe a wide range of different physical conditions in the interstellar medium and nebulae. The UV grism will enable low-resolution (R~200) slitless spectroscopy over the spectral range ~200 - 400 nm.

3.4 Operating Modes

The UVIS channel single observing mode is called "ACCUM", the configuration in which photons are counted on the WFC3 CCD detectors as accumulated charge. The charge is read-out at the end of an exposure, converted to Data Numbers (DN) at a pre-defined gain, stored in a data memory array, and, when the array is full, dumped to the science data recorder onboard HST.

In addition to a full array image, the user can request sub-array or binned images. A suite of fixed, pre-defined subarray apertures are available to the GO as well as a limited capability for user-defined subarrays. The subarray option is best suited to minimize data volume and read-out time for time-sensitive observations such as observations of bright point sources, solar systems objects or rapidly varying objects.

The binning option, 2 by 2 or 3 by 3, allows for better surface brightness sensitivity during low-background observations (e.g. narrow-band or UV imaging) by reducing the relative contribution from read-out noise in cases

when maximum resolution is of secondary importance. Binning will also reduce the data volume.

Users can select among a suite of standard dithering patterns, which includes both integer and sub-pixel shifts, obtained by moving the telescope (note, though, that integer pixel shifts can effectively take place only over relatively small portions of the field of view because of geometrical distortions). These patterns help improve the effective resolution by allowing the user to improve the sampling of the PSF by suitable combination of the dithered images (drizzling) while at the same time minimizing the effects of detector cosmetic defects.

4. The IR Channel

The IR Channel is optimized over the wavelength range 850-1700nm. The IR optics, with the exception of the WFC3 pick-off mirror (which intercepts the central bundle of light from the OTA and is shared with the UVIS channel) are coated with a protected silver coating for maximum IR throughput. The IR channel consists of the Channel Select Mechanism (CSM) which diverts the light from the UVIS channel optical train, a separate mechanism providing focus and alignment adjustment, elements for spherical aberration correction, a Filter Selection Mechanism (FSM), and a HgCdTe detector assembly. The IR optical chain is supported by a thermal control subsystem and also by control and data-handling electronic subsystems. The correction for the spherical aberration from the HST primary mirror is done by a refractive corrector plate (RCP). Since the detector is electronically shuttered, a shutter mechanism is not part of the IR channel design, and bright-object protection is obtained by blocking the optical path with an opaque slot in the Filter Selection Mechanism.

4.1 Field of View and Pixel Size

The pixel size of the IR channel, selected by the SOC after careful analysis, is the result of an optimal balance between field of view and PSF quality. Simulations have shown that dithering and image reconstruction techniques (drizzling) are able to reconstruct a good quality PSF satisfactorily as long as the pixel size is below 0.15 arcsec. The final choice of approximately 0.13 arcsec satisfies this requirement while at the same time satisfying optical packaging considerations. Since the focal plane is tilted by about 22 degrees with respect to the chief ray, the field of view is rectangular in shape, with an aspect ratio of ~0.89. The scale of the rectangular pixels is 0.121 x 0.135 arcsec, which yields a useful field of view with size 123 x 137 arcsec.

4.2 IR Detector Array

The WFC3 IR detector is a HgCdTe 1024 x 1024 array of 18.0 x 18.0 μm pixels bonded on a silicon multiplexer (MUX). Of these, the inner 1014 x 1014 pixels are light sensitive and are used for imaging, while the bordering 5 pixels around each side of the array provide a constant-voltage reference and are used for accurate subtraction of the electronic bias. This device is a direct descendant of the NICMOS 256 x 256 and Hawaii 1024 x 1024 arrays, widely used in astronomy. To eliminate the complication and the limited lifetime of a stored cryogen system while at the same time provide the low operating temperatures required for dark current and thermal background reduction, the WFC3 IR detector is cooled with a six-stage thermoelectric cooler to a nominal operating temperature of 150 K. The array sensitivity is optimized in the spectral interval 850-1700 nm. A cutoff value of 1700 nm has been chosen to limit the "effective" dark current (i.e. the sum of the intrinsic detector dark current and the instrument internal background), given the restrictions imposed by the operating temperature. A longer cutoff wavelength would increase the effective dark current at a given detector temperature because of the background due to thermal emission from the telescope and the optical bench.

The currently selected flight detector has a read-out noise of about 16 electrons rms after multiple reads. The sum of detector dark current and thermal background contributions is predicted to be lower than the requirement of 0.4 electrons per pixel per second. These values of the detector read-out noise and dark current will allow zodiacal background limited imaging in both the J and the H band (1600 nm).

Finally, the Modulation Transfer Function (MTF) is expected not to broaden the PSF by more than 10 per cent. The intrinsic photometric accuracy is expected to be better than 5 per cent.

4.3 Internal and OTA Thermal Background

Given the overall design of the IR channel, particular care has been put into minimizing the thermal background contribution to the detector effective dark current and reducing the thermal load on the detector. As mentioned earlier, this has been achieved by cooling the optical bench, by designing a cooled, baffled camera head for the IR detector, and by including a cold stop mask in the design. This latter component greatly decreases both the thermal load and the effective background coming from the instrument itself and its parts and from the HST OTA, meeting the goal of 0.2 electrons/sec/pixel in the H band with a detector cut-off of 1760 nm, at the cost of a modest loss of throughput of the order of 10%. Since the contribution to the background by the zodiacal light is ~0.2 electrons/sec/pixel in the H band, the instrument will meet the goal of

being near background (i.e. zodiacal light) limited in this passband. A similar performance is achieved in the J band. The filter wheel is also cooled to reduce the contribution to the background due to the potentially high off-band emissivity of the filters.

4.4 Spectral Elements

The IR channel Filter Selection Mechanism has 18 slots and contains 15 passband filters, two grisms, and a blank position. The filter complement, which has been recommended by the SOC with broad community input, covers the extended range 850 nm to 1700 nm and includes broad-band filters, medium-band filters centered on molecular lines and the nearby continuum, and narrow-band filters probing interstellar diagnostic lines. Table 5 lists the name and the main characteristics of the IR spectral elements.

The J and H filters have conventional values of the central wavelengths for these passbands, namely 1250 and 1600 nm; however, although the J-band filter has a width comparable to that of a typical passband used in ground-based cameras, the width of the H-band filter has been modified to better fit the quantum-efficiency curve of the detector. Specifically, the H filter is narrower to limit thermal background and to have its transmittance define the effective bandpass at the red end rather than the detector quantum efficiency. This arrangement minimizes photometric instability due to variations in the detector's characteristics (e.g. induced by temperature fluctuations). The instrument includes also a wide J-band filters (F110W) similar to the corresponding filter in NICMOS. The two grisms will provide WFC3 with the ability to take slitless spectra of sources at a resolving power of about 140 in the wavelength range 1100 to 1700 nm, and of about 200 in the 900 to 1100 nm range.

4.5 Operating Modes

The operational mode for the IR channel, MULTIACCUM, begins with an array reset followed by two rapid contiguous read-outs. Next one or more non-destructive readouts are obtained at various intervals, depending on the type of sample sequence and number of samples (up to a maximum of 16) requested by the user. All 16 reads (including the initial two) are recorded and returned to the ground for analysis

On-orbit experience with NICMOS shows that non-destructive readout is a very effective readout mode, because it reduces the effective readout noise and corrects for most cosmic-ray hits. Many IR observations are expected to make use of sub-pixel dithering to improve the PSF sampling. Suitable dithering patterns are included in the proposal software tools (APT) and can be commanded by the observer. The IR channel also supports sub-array readout modes to allow for the short integration times required by bright targets (e.g. the HST standard stars and solar system planets) and to reduce data volume.

5. Observing with WFC3

5.1 Overview

When planning observations with WFC3, observers should carefully evaluate the capabilities of the instrument and compare them to those of other similar HST instruments to identify the best observational strategy for their scientific goals. While such a comparison should include all imagers on board of HST, ACS and NICMOS must receive particular attention because WFC3 intentionally provides redundancy of functions with these instruments (to protect against failures that would compromise HST's imaging capabilities); however it also differs sufficiently from (in fact, it largely complements) them that observers need to carefully consider the relative capabilities to optimize their observations. Table 3 lists the primary characteristics of the imaging science instruments that will be onboard HST after SM4. The four factors to consider are areal coverage, resolution, wavelength coverage and throughput.

For some research programs, the choice of the instrument may be dictated by the need of a particular spectral element, and in this regard WFC3 offers great flexibility, since it features ample choice of broad-, medium-, and narrow-band filters both at UV/optical and near-IR wavelengths as well as a UV prism and two near-IR grisms for slitless spectroscopy at low resolution (see Table 4 and Table 5 below).

For studies at optical wavelengths, the trade-offs to consider when deciding between WFC3/UVIS and ACS/WFC are between pixel size, field of view and, to some extent, throughput. WFC3 is preferred when angular resolution has higher priority over field of view. ACS/WFC has ~20% higher throughput than WFC3/UVIS around the center of the optical window (see Figure 2), and hence it should be used whenever the highest sensitivity at these wavelengths is crucial for the observations. However, considerations of charge-transfer efficiency (CTE) should also be kept in mind, since ACS will be at least two years old when WFC3 comes on line, and the CTE of its CCD will have suffered some amount of degradation due to radiation damage.

At UV wavelengths, WFC3/UVIS is the only imager on HST to offer a large FOV coupled with high throughput. However, its spectral coverage ends at 200 nm, while ACS/SBC and STIS/FUV-MAMA reach 115 nm (STIS/NUV-MAMA reaches 160 nm) and also offer higher spatial sampling (see Table 2 and Table 3). Thus, WFC3 will be the choice whenever large field of view and coverage to the far-UV spectral range are simultaneously required (e.g. multi-wavelength surveys). If observations at extreme far-UV wavelengths are necessary or if the highest available spatial sampling is a primary requirement, then ACS/HRC, ACS/SBC or the STIS UV channels should be considered.

At near-IR wavelengths WFC3/IR offers a much larger field of view and, generally, higher throughput over NICMOS. It also offers improved effective sensitivity and ease of data reduction and calibration due to the accurate pedestal subtraction made possible by the presence of reference pixels. However, WFC3 sensitivity is limited to wavelengths bluer than about 1700 nm, and WFC3 has larger pixel sizes than NIC1 or NIC2.

Table 3: . Primary characteristics of the HST imaging Science Instruments after SM4. * Value for the flight candidate detector.** This value includes the instrument thermal background

Instrument	Wavelength Range, nanometers	Pixel Size, arcsec)	FOV, arcsec^2)	Read-out noise (single read), e$^-$ rms	Dark current, e$^-$/pix/s
ACS/HRC	200-1050	0.026	26 x 26	5	0.003
ACS/WFC	350-1050	0.050	205 x 205	5	0.002
STIS/CCD	200-1050	0.050	52 x 52	4.9	0.003
NICMOS/CAM2	800-2500	0.076	19 x 19	35	0.4
NICMOS/CAM3	800-2500	0.200	51 x 51	35	0.4
WFC3/UVIS	**200-1000**	**0.040 x 0.040**	**163 x 162**	**4**	**<0.0056**
WFC3/IR	**850-1700**	**0.121 x 0.135**	**123 x 137**	**16***	**<0.4****

Finally, an important thing to remember is that the capability of the HST-ground data link to support simultaneous operations of WFC3 and ACS as well as possible solutions to increase its bandwidth are still being evaluated as of this writing. Whether it will be possible to allow parallel observations with these two instruments, therefore, is not known at this time.

5.2 Spectral Elements

The spectral elements have been chosen to cover many scientific problems, from color selection of distant galaxies to accurate photometry of stellar sources to narrow-band imaging of nebular gas. The filter suite for WFC3 was defined by the Scientific Oversight Committee with input from the astronomical community. To reflect the importance of the blue wavelength regime and the high blue sensitivity of the WFC3 UVIS channel, several blue filters are included in the UVIS filter set. Spanning the entire wavelength region are filters consistent with the WFPC2, ACS, and NICMOS sets, and the Sloan photometric system. The shape of the passband of some specific filters has been designed for specific purposes, such as providing maximum throughput (e.g. some UV filters) or matching the response of the detector to provide photometric stability (e.g. the H band in the IR channel). Table 4 and Table 5 list the available passbands for the UVIS and IR channels and their characteristics.

Table 4: WFC3 UVIS Filters

Name	Description	Central λ[1] (Å)	Width[2] (Å)	Pivot λ[3] (Å)	Peak Transmission	Mean λ[4] (Å)
F218W	ISM feature	2202.1	306.9	2219.0	0.36	2204.8
F225W	UV Wide	2263.2	475.4	2284.3	0.32	2256.1
F275W	UV Wide	2743.6	590.0	2742.4	0.36	2713.3
F300X	Long Pass	2764.5	827.4	2819.6	0.45	2747.4
F336W	U, Stromgren u	3358.2	553.8	3361.1	0.75	3345.8
F350L	Long Pass	(5800)[5]	(4500)[5]	6812.0	0.98	5447.6
F390M	Long Pass	3896.4	210.5	3893.8	0.88	3891.5
F390W	Washington C	3895.4	953.0	3904.6	0.96	3862.4
F410M	Stromgren v	4109.6	198.7	4111.6	0.66	4109.7
F422M	continuum	4218.6	113.3	4217.7	0.69	4217.1
F438W	WFPC2 B	4306.2	676.8	4318.7	0.84	4300.5
F467M	Stromgren b	4688.7	246.7	4690.2	0.82	4687.9
F475W	SDSS g	4704.7	1488.9	4760.6	0.92	4684.9
F475X	Long Pass	4779.1	2199.6	4917.1	0.94	4732.9
F547M	Stromgren y	5451.6	714.0	5447.0	0.88	5431.3
F555W	WFPC2 V	5206.2	1595.1	5309.8	0.95	5206.6
F600L	Long Pass	(7900)[5]	(4000)[5]	8402.2	1.00	7933.6
F606W	WFPC2 Wide V	5840.5	2345.0	5932.3	0.96	5782.6
F621M	11% passband	6207.4	650.8	6212.0	0.94	6200.3
F625W	SDSS r	6224.8	1575.4	6254.0	0.95	6187.4
F689M	11% passband	6875.5	708.6	6886.0	0.94	6873.3
F763M	11% passband	7632.2	798.6	7636.3	0.97	7622.3
F775W	SDSS i	7707.5	1486.0	7733.6	0.85	7685.2
F814W	WFPC2 Wide I	8235.9	2543.3	8304.7	0.97	8174.4
F845M	11% passband	8458.5	886.7	8468.9	0.96	8452.8
F850L	SDSS z	(9400)[5]	(1500)[5]	9756.4	0.96	9652.5
F232N	CII] 2326	2326.3	32.2	2326.9	0.12	2326.8
F243N	[NeIV] 2425	2420.3	34.8	2420.6	0.15	2420.5
F280N	MgII 2795/2802?	2796.1	39.5	2796.1	0.21	2796.0
F343N	[NeV] 3426	3377.7	140.0	3438.0	0.78	3433.5
F373N	[OII] 3726/29	3728.1	39.2	3729.6	0.78	3729.5
F378N	z ([OII] 3727)	3787.8	89.2	3790.9	0.83	3790.4
F387N	[NeIII] 3869	3871.5	23.1	3873.0	0.72	3872.9
F395N	CaII H&K	3952.8	72.9	3953.7	0.86	3953.3
F436N	[OIII] 4363	4366.5	35.7	4366.7	0.67	4366.6
F437N	[OIII]4353	4370.7	24.6	4370.6	0.70	4370.6

Name	Description	Central λ[1] (Å)	Width[2] (Å)	Pivot λ[3] (Å)	Peak Transmission	Mean λ[4] (Å)
F469N	HeII 4686	4685.3	37.2	4687.5	0.69	4687.4
F487N	H-b 4861	4869.0	48.4	4870.7	0.85	4870.5
F492N	z (H-b)	4930.6	101.0	4932.1	0.85	4931.6
F502N	[OIII] 5007	5008.3	57.8	5009.0	0.87	5008.8
F508N	z ([OIII] 5007)	5089.5	117.9	5089.7	0.87	5089.1
F575N	[NII] 5755	5756.3	12.9	5755.9	0.78	5755.9
F588N	HeI 5876	5881.7	59.7	5882.2	0.88	5882.0
F619N	CH4 6194	6197.1	61.6	6197.5	0.89	6197.3
F631N	[OI] 6300	6306.5	43.1	6303.0	0.86	6302.9
F634N	6194 cont.+	6346.7	66.2	6347.5	0.88	6347.4
F645N	Continuum	6451.9	85.0	6451.6	0.86	6451.5
F656N	H-a 6563	6561.0	13.9	6561.1	0.86	6561.1
F657N	Wide Ha+[NIII]	6557.3	96.3	6565.1	0.90	6564.6
F658N	[NII] 6583	6584.8	13.7	6587.2	0.79	6587.2
F665N	z (Ha +[NII])	6656.8	109.0	6654.4	0.90	6653.9
F672N	[SII] 6717	6716.0	14.9	6716.1	0.89	6716.1
F673N	[SII] 6717, 31	6759.3	100.5	6764.5	0.91	6764.1
F674N	[SII] 6731	6729.5	10.0	6729.5	0.68	6729.5
F680N	z (Ha +[NII])	6874.1	323.6	6878.6	0.95	6875.0
F727N	CH4 7270	7274.5	64.8	7274.7	0.89	7274.6
F750N	7270 cont.	7500.4	68.8	7500.6	0.85	7500.5
F889N	25/km-agt	8891.3	93.7	8891.8	0.90	8891.6
F906N	2.5/km-agt	9057.5	94.0	9056.7	0.92	9056.5
F924N	0.25/km-agt	9246.2	89.2	9246.3	0.94	9246.0
F937N	0.025/km-agt	9370.7	91.9	9371.1	0.91	9370.9
F953N	[SIII] 9532	9530.2	84.6	9529.7	0.90	9529.5

1. Central Wavelength defined as geometric mean wavelength.
2. FWHM (T=+/-50% wavelengths for wide/medium bands and T=+/-90% wavelengths for narrow bands.
3. Pivot Wavelength defined as the "center of mass" of the filter weighted by the inverse wavelength.
4. Mean wavelength defined as half way between the frequency and wavelength means of the filter.
5. For Long Pass Filters, values are approximate central λ and widths using throughput convolved with detector QE.

Note: Wide Bands measured in 10Å increments (1.0Å accuracy) Narrow bands measured in 1Å increments (0.1Å accuracy).

Table 5: WFC3 IR Filters

Name	Description	Central λ[1] (nm)	Width[2] (nm)	Pivot λ[3] (nm)	Peak Transmission	Mean λ[4] (nm)
F093W	Wide Band passes 633nm	836.18	464.58	827.37	0.99	827.37
F105W	Wide FAT "z	1052.11	292.30	1048.95	0.98	1048.95
F110W	Wide J (equal H area)	1148.06	501.12	1137.75	0.99	1137.75
F160W	Broad H and Red Grism Ref *	1543.17	287.88	1540.52	0.98	1540.52
F125W	Broad J	1248.68	297.77	1244.94	0.98	1244.94
F098M	"Blue" Filter, Blue Grism Ref *	984.72	169.48	982.93	0.97	982.93
F127M	Water/CH_4 continuum	1273.55	68.79	1273.64	0.98	1273.64
F139M	Water/CH_4 line	1383.62	64.58	1383.80	0.98	1383.80
F153M	H_20 and NH_3	1533.24	68.78	1533.31	0.98	1533.31
F126N	[FeII]	1258.28	11.83	1258.26	0.90	1258.26
F128N	Paschen Beta	1283.36	13.54	1283.30	0.94	1283.30
F130N	Paschen Beta continuum	1300.58	13.28	1300.62	0.96	1300.62
F132N	Paschen Beta (redshifted)	1319.08	13.07	1319.04	0.91	1319.04
F164N	[FeII]	1645.22	17.48	1645.13	0.93	1645.13
F167N	[FeII] continuum	1667.18	17.16	1667.26	0.93	1667.26
G141	"Red" Low Resolution Grism	(14100)[5]	(6000)[5]			
G102	"Blue" High Resolution Grating	(10250)[5]	(2500)[5]			

1. Central Wavelength defined as geometric mean wavelength.
2. FWHM (T=+/-50% wavelengths).
3. Pivot Wavelength defined as the "center of mass" of the filter weighted by the inverse wavelength.
4. Mean wavelength defined as half way between the frequency and wavelength means of the filter.
5. Grism values are requirements, not as-built.

5.3 WFC3 Sensitivity

WFC3's cameras (detectors, optical elements, and spectral elements) have been designed to provide the highest possible sensitivity, while also fulfilling the requirement of wide spectral coverage, extending from the redder end of the far UV region to the bluer end of the near IR. As a result of this design requirement, the sensitivity of WFC3 UVIS does not reach the peak value of ACS/WFC in the R band, although it is still very high in absolute terms and remarkably flat overall from 200 to 1000 nm. At near infrared wavelengths, WFC3/IR generally offers higher throughput than NICMOS over the wavelength range in common (see Figure 2). Table 6 compares the sensitivity of both channels of WFC3 to that of the analogous cameras of ACS and NICMOS.

At the time of this writing, the flight IR detector is still being assembled and its performance needs to be fully characterized with the flight electronics. Thus, values for the detector noise parameters are subject to

change. Figure 7 shows the quantum efficiency of the current detectors of the two channels of WFC3 as a function of wavelength. For the UVIS channel the curves of each CCD are shown; for the IR channel the figure shows an average curve across the array. Table 6 lists a range of sensitivity values obtained in one case under the assumption that the delivered detector meets the original specification requirements, namely a read out noise of 15 e- rms, and in the other case that the detector has read out noise of 30 e- rms, labeled as "15" and "30", respectively, in the table (all cases are single read; a reduction of the noise of a factor of 2 has been assumed in both cases as a result of the adoption of the MULTIACCUM sequence).

Table 6: Summary of WFC3 performance compared to ACS-WFC and NICMOS-NIC3.Columns 2 and 4 list the exposure time required to reach S/N=10 for a stellar and resolved source, respectively. Columns 3 and 5 list the limiting magnitude (in the HST f_λ magnitude system) with S/N=5 in a 10-hr exposure (30 exposure of 20 minutes each have been assumed). An aperture of 0.5 arcsec diameter has been assumed for diffuse sources. In all cases a spectral energy distribution proportional to λ^{-2} (in units of erg/sec/cm^2/Å) has been used in the calculation..

	S/N=10 Stellar	Limiting mag Stellar, 10 hr	S/N =10 Diffuse	Limiting mag Diffuse, 10 hr
WFC3 UVIS	V=20, 1.6 sec	V=28.3	V=20, 2.8 sec	V=27.5
ACS WFC	V=20, 1.1 sec	V=29	V=20, 2.0 sec	V=27.7
WFC3 IR (15)	H=20, 9.3 sec	H=27.0	H=20, 17.6 sec	H=26.3
WFC3 IR (30)	H=20, 17.1 sec	H=27.0	H=20, 33.0 sec	H=26.0
NICMOS-3	H=20, 21 sec	H=26.4	H=20, 21 sec	H=26.4

In order to help in the instrument development, the IPT maintains an exposure-time calculator (ETC) for both channels. This ETC is not meant to be used for proposal preparation. The ETC can be found at the URL:
http://www.stsci.edu/instruments/wfc3/etc-list.html.

The present ETC will be superseded by a more general software tool included in the Astronomer Proposing Tool (APT) before the release of the call for proposal for Cycle 14.

Figure 4: Integrated system throughput of WFC3 UVIS long pass, broad and medium band filters. The curves include the HST OTA, WFC3 UVIS internal throughput, the filter transmittance, and the QE of the UVIS detector.

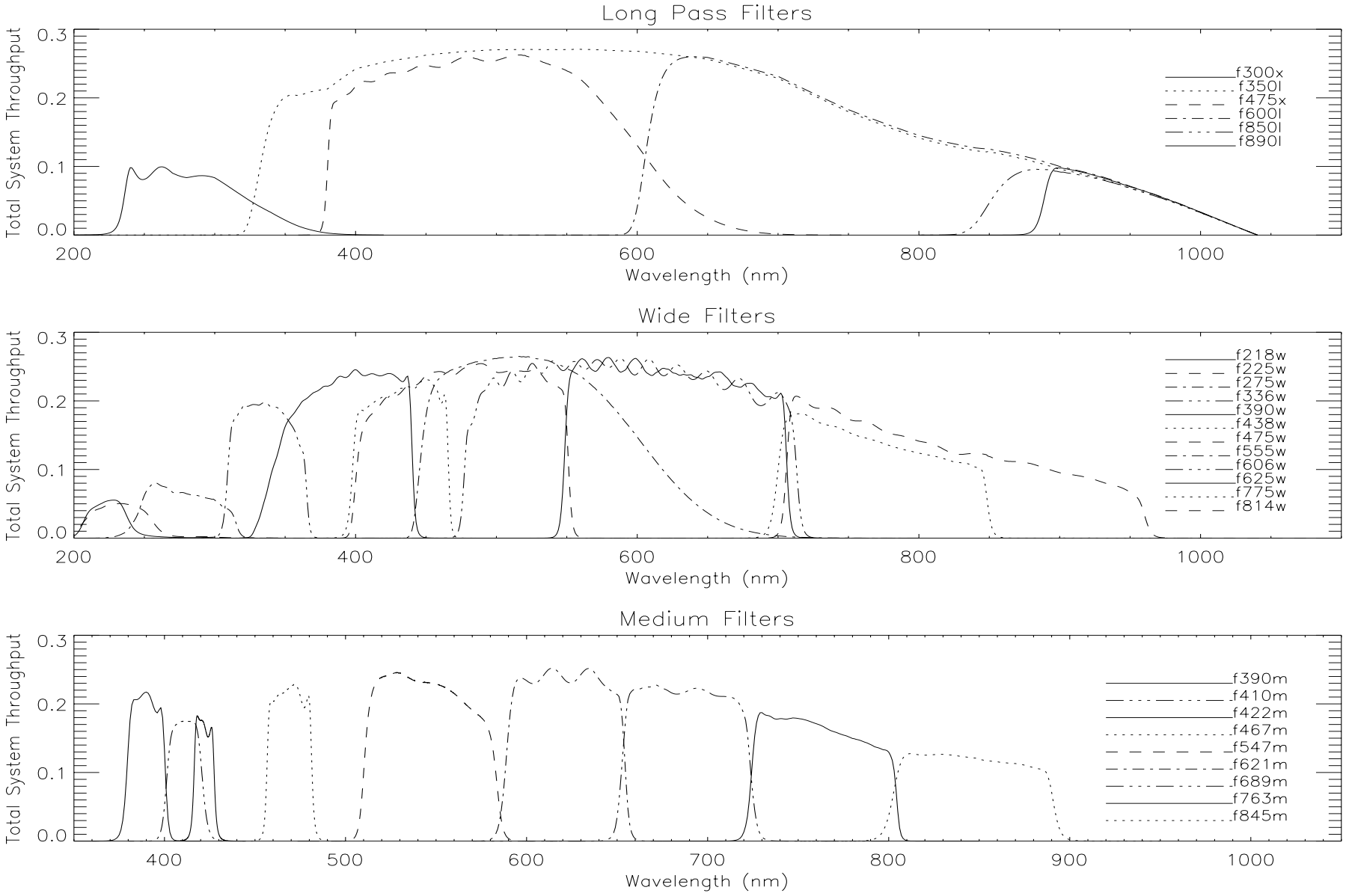

Figure 5: Integrated system throughput of WFC3 UVIS narrow band filters. The curves include the HST OTA, WFC3 UVIS internal throughput, the filter transmittance, and the QE of the UVIS detector

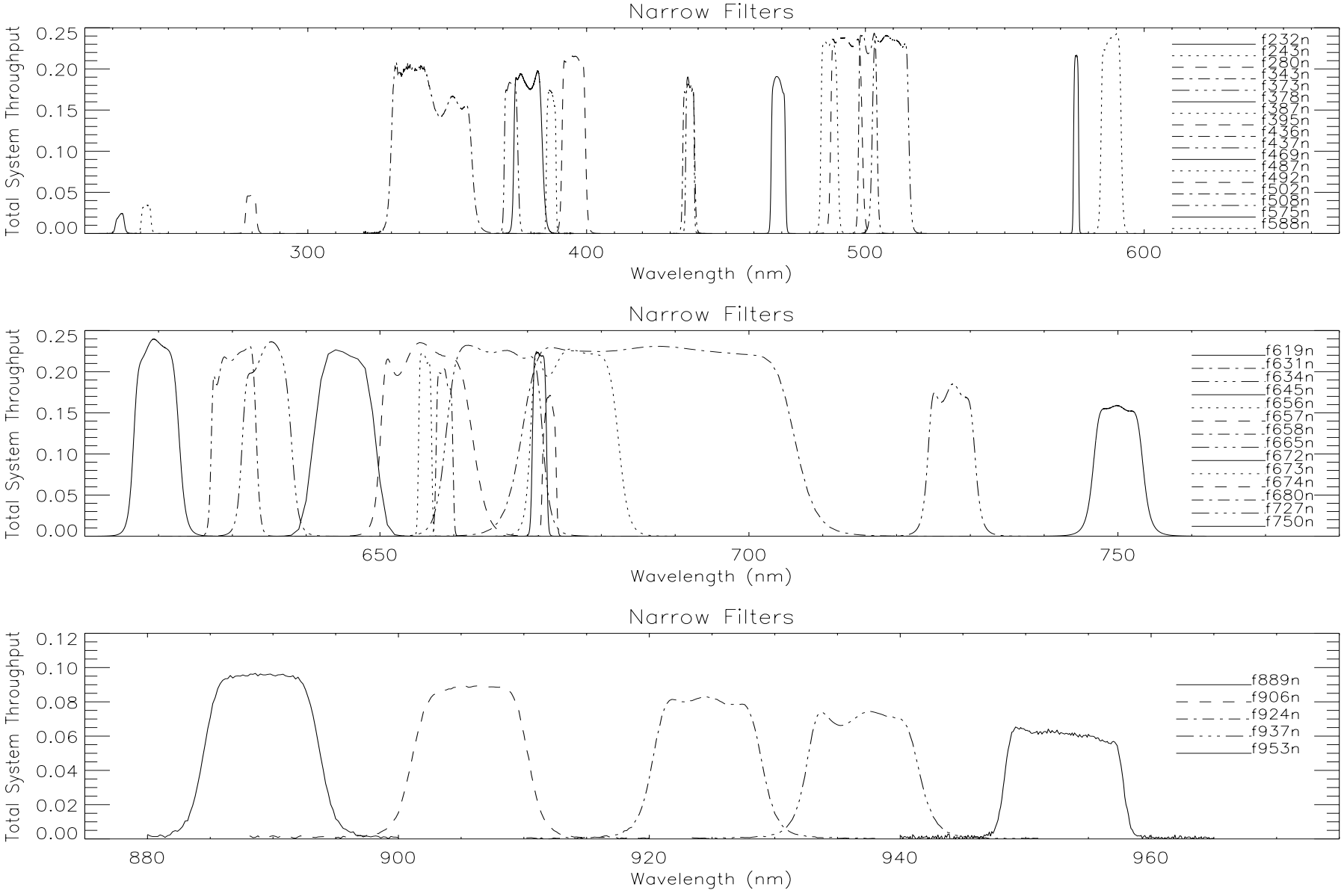

Figure 6: Integrated system throughput of WFC3 IR long pass, broad, medium, and narrow band filters. The curves include the HST OTA, WFC3 IR internal throughput, the filter transmittance, and the QE of the IR detector.

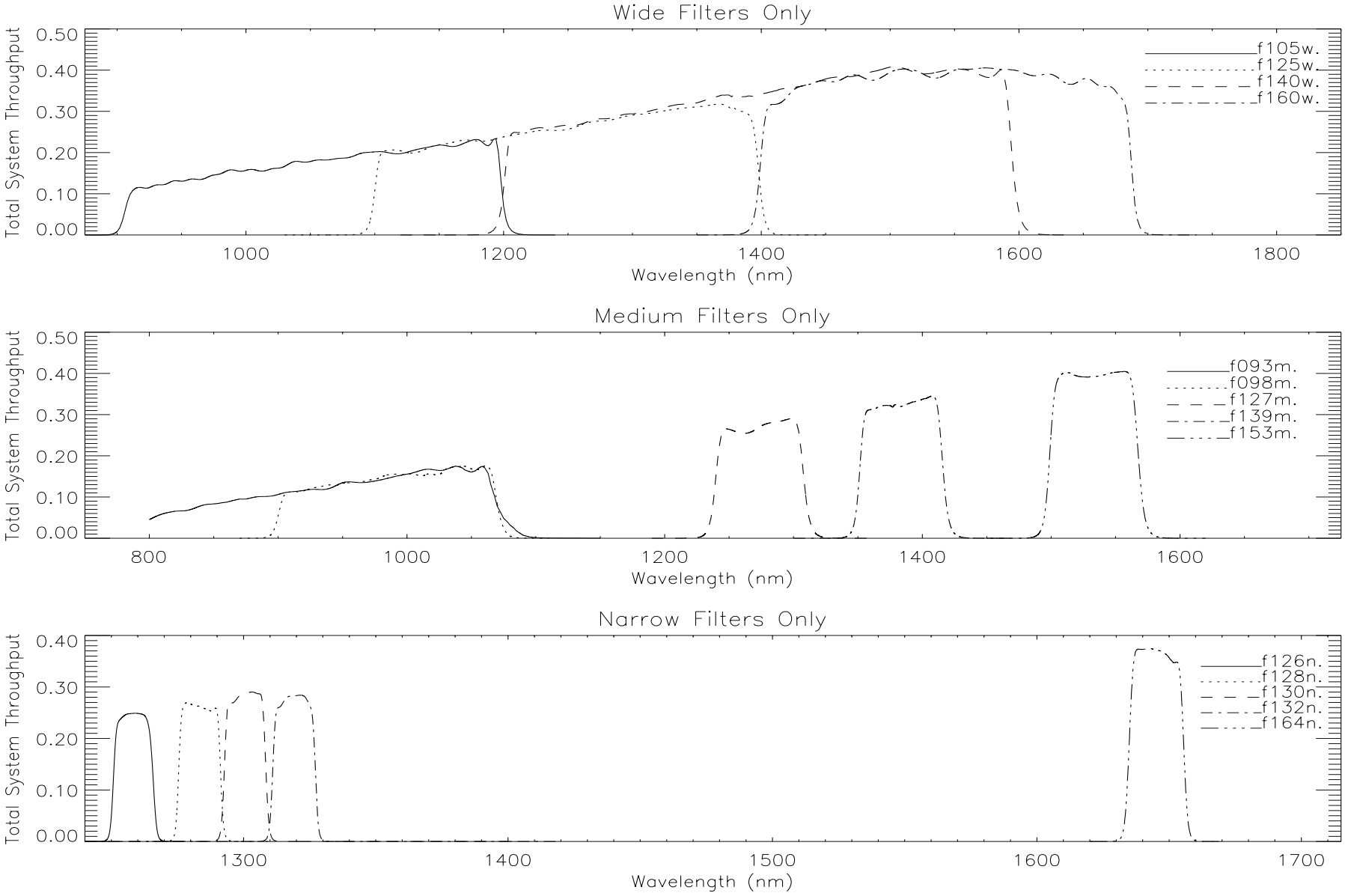

Figure 7: The quantum efficiency of the detectors of WFC3. The continuous curves show the measured quantum efficiency of the detectors currently adopted as flight parts. For the UVIS channel, the curves of both CCD chips of the array are shown, while the curve for the IR channel is the average of four quadrants of the array. The dashed curves show the quantum efficiency specifications submitted to the manufacturers by the WFC3 project (lower curves are the minimum, upper curves the goal).